PCCP

PAPER

View Article Online
View Journal | View Issue

Cite this: *Phys. Chem. Chem. Phys.*, 2025, **27**, 8856

The reaction of sulfenic acids with OH and HO_2 radicals in different environments†

Josep M. Anglada, *[a] Ramon Crehuet, *[a] Marilia T. C. Martins-Costa,[b] Joseph S. Francisco [c] and Manuel F. Ruiz-López [b]

Received 25th October 2024,
Accepted 31st March 2025

DOI: 10.1039/d4cp04106b

rsc.li/pccp

Sulfenic acids are involved in major chemical processes occurring in the atmosphere, in food chemistry and in biological systems. In these diverse environments, oxidation reactions caused by reactive oxygen species, especially hydroxyl (OH) and hydroperoxyl (HO_2) radicals, are very important, but their mechanisms remain poorly understood. To address this question, in this paper we present high-level theoretical results on selected reactions in gas phase and in aqueous solution. The study shows that the abstraction of the acidic hydrogen by OH or HO_2 is the most important process in all cases. It leads to the formation of sulfinyl radicals and H_2O or H_2O_2, respectively, following a proton-coupled electron transfer (pcet) mechanism. The associated rate constants depend on sulfenic acid derivative when the oxidizing species is HO_2, but all processes are diffusion controlled in the case of reaction with OH. From structurally simple systems to a cysteine-derived model peptide, this work provides a systematic study that contributes to a comprehensive understanding of the reactivity of sulfenic acids with radicals.

Introduction

Oxidation reactions are ubiquitous and play key roles in the chemistry of the atmosphere, in environmental chemistry and in biological systems. Among the most important oxidants in all these environments, the hydroxyl (OH) radical, the hydroperoxyl (HO_2) radical and its associated superoxide anion O_2^-, hydrogen peroxide (H_2O_2) and ozone (O_3) have special relevance and are commonly classified as reactive oxygen species (ROS). In the atmosphere, the gas-phase chemistry of the HO_x radicals and ozone prevails. In living organisms, ROS can originate from pollutants in the environment,[1,2] but they can also have an endogenous origin, initiated by electron reduction of molecular oxygen.[3] They have important biological signaling activities, but cause oxidative stress when dysfunction within the antioxidant system occurs.[4–6] Excess ROS in living organisms can lead to problems such as protein oxidation, through either cleavage of the polypeptide chain or modification of amino acid side chains, and lipid oxidation.[3,7,8] The chemistry of ROS in the atmosphere and in biological systems has many similarities despite the different composition and thermodynamic conditions between these media, and this similarity has been discussed by bringing in data across the literature to highlight the common chemistry connections to all of these systems and chemical reaction environments.[2] Here we report on our study of the reactivity of sulfenic acids with ROS species (*i.e.* OH and HO_2) across different reaction environments, namely gas- and solution-phases.

Sulfenic acids (R-SOH) have been of keen interest for more than three-quarters of a century and play important roles in different environments. They have been found to be key reaction intermediates in organic and bioorganic sulfur chemistry, as they can exhibit both nucleophilic and electrophilic character.[9,10]

In the atmosphere, dimethyl sulfide (CH_3SCH_3, DMS)[11] and dimethyl disulfide (CH_3SSCH_3, DMDS)[12] are major sources of atmospheric sulfur, with a great impact on the formation of aerosols, on climate and on air quality.[13–15] The atmospheric oxidation of DMS and DMDS are mainly initiated by OH and the major products are methane sulfonic acid and sulfur dioxide, which further reacts with OH and H_2O leading to sulfuric acid. However, between 3% and 7% of the DMS oxidation product forms methane sulfenic acid (CH_3SOH, MSEA),[16,17] and about 98% of the oxidation of DMDS by hydroxyl radical produces MSEA.[18–20] Indeed, methane sulfenic acid is quite stable in the gas phase[21] and has been characterized by microwave spectroscopy, by photoelectron spectroscopy, and by Fourier transform infrared spectroscopy,[19,21,22] and its photochemistry has recently been investigated.[23] However, its reactivity remains largely unexplored, with the exception of its reaction

[a] *Institute for Advanced Chemistry of Catalonia (IQAC) – CSIC, c/Jordi Girona 18-26, E-08034 Barcelona, Spain. E-mail: anglada@iqac.csic.es, rcsqtc@iqac.csic.es*
[b] *Laboratoire de Physique et Chimie Théoriques, UMR CNRS 7019, University of Lorraine, CNRS, BP 70239, 54506 Vandoeuvre-lès-Nancy, France*
[c] *Department of Earth and Environmental Science and Department of Chemistry, University of Pennsylvania, Philadelphia, PA, USA 19104-6316*

† Electronic supplementary information (ESI) available. See DOI: https://doi.org/10.1039/d4cp04106b

with ozone.[20] Consequently, investigating the reactions of MSEA with OH and HO_2, two of the primary atmospheric oxidants, is of significant interest.

In food chemistry, allium plants such as garlic, onion, leeks and shallots are known to play important roles in cure and prevention of human diseases, including bacterial, viral and fungal infections. These plants also show antioxidant, anti-blood pressure or even anticancer properties, which are mostly attributed to the sulfur compounds they contain, with sulfenic acids among them.[24,25] In particular, the enzyme alliinase catalyzes the cleavage of *S*-allyl-L-cysteine S-oxide (in garlic)[9] or *S*-alkenylcysteine S-oxide (in onion)[26] producing 2-propenesulfenic acid (CH_2═CH–CH_2SOH) and 1-propensulfenic acid (CH_3–CH═$CHSOH$), respectively. These acids are potent antioxidants,[27–31] having a much greater radical scavenger abilities than other sulfur compounds.[32] It is worth mentioning that when onions are cut their cells are broken and release the enzyme alliinase and water, which react with *S*-alkenylcysteine S-oxide, producing 1-propenesulfenic acid. The oxidation of this sulfenic acid by lachrymatory factor synthase leads to the formation of *syn*-propanethial S-oxide (CH_3CH_2CHSO), which irritates the lachrymal glands, causing tears when peeling onions.[26]

Sulfenic acids are also formed by the oxidation of thiol groups (–SH),[33] such as the cysteine residues of proteins,[34] or by the oxidation of cysteine disulfides by hydroxyl radical. They play an important role in enzyme catalysis, redox homeostasis, and cell signaling.[35–38] Consequently, they are crucial in the regulatory system and in combating elevated concentration of reactive oxygen species (ROS) under oxidative stress conditions.[8,39] Sulfenic acids can also be formed by a two electron oxidation mechanism involving hydrogen peroxide, superoxide anion, hydroperoxides, nitric oxide, peroxynitrite, by hydrolysis and oxidation of disulfides or by reaction with monooxygenases.[7,37,40,41] Sulfenic acids can either act as nucleophiles or electrophiles,[36,37] reacting with hydrogen peroxide, thiols, thiolates, amines and others,[42–47] and also act as radical trapping species.[8,28–31] It has also been proposed that protein–SOH intermediates react with a secondary thiol group leading to the formation of a disulfide bond.[36,37,48] However hydroxyl radical can also react with disulfide bonds leading to the back formation of sulfenic acids.[37,41] Very interestingly, it has recently been shown that sulfenic acid can activate the decomposition of H_2O_2 producing OH radicals.[49] Little is known about the evolution and degradation of these sulfenic acids, and we hypothesized that oxidation with HO_x could be a relevant degradation route.

In this work we investigate the affinity of sulfenic acids **1** to **4** (Scheme 1) with OH and HO_2 (HO_x) radicals, both in gas phase and in water solvation. Compounds **1**, **2**, and **3** are important species in the atmosphere, in garlic, and in onion, respectively, whereas compound **4**, which includes two peptide bonds, is chosen to model the sulfenic acid that would arise from oxidation of cysteine side-chain in proteins.

The goal is to provide insight into the molecular drivers behind the reactivity of sulfenic acids with OH and HO_2 radicals, from fundamental, structurally simple sulfenic acids to more complex systems, and to develop a common reactivity scale that crosses atmospheric, environmental, and biological media, where this chemistry takes place.

Theoretical methods

All the reactions between compounds **1**, **2**, and **3** with OH and HO_2 radicals have been investigated, in a first step, with the M06-2X[50] density functional using the 6-311+G(2df,2p) basis set.[51] In a second step, and in order to obtain accurate relative energies, we have performed single-point energy calculations at the optimized geometries using different theoretical approaches, depending on the system, namely:

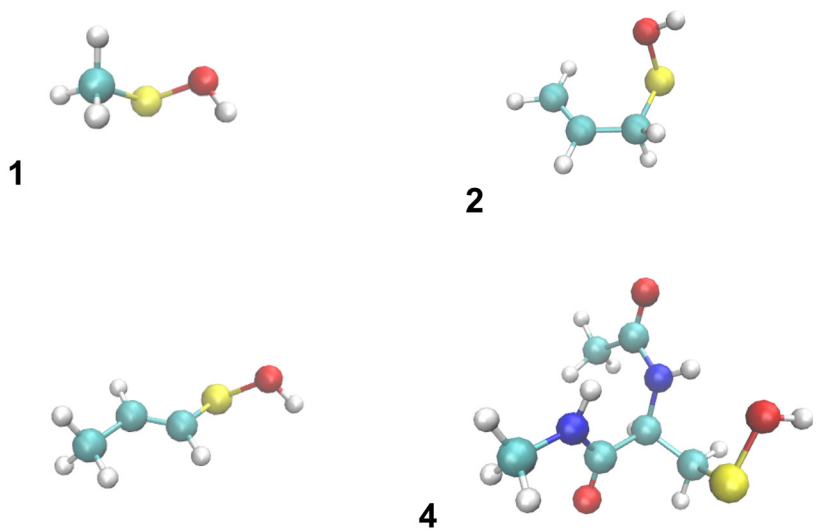

Scheme 1 Sulfenic acids considered in this work.

(1) The domain-based local pair natural orbital coupled cluster including perturbative triplet excitation DLPNO-CCSD(T)[52] method with the aug-cc-pVTZ basis set,[53] and

(2) the coupled cluster method with single and double excitations, and a perturbative treatment of all connected triplet excitations CCSD(T) method[54] employing the aug-cc-pV(T+d)Z, aug-cc-pV(Q+d)Z and complete basis set (CBS) limit.[51,53,55–57]

For the reaction of compound **4** with OH and HO_2 radicals, the computational methods employed include a combination of molecular mechanics (MM) methods,[58] *ab initio* density functional theory with the M06-2X density functional approach followed by single point energy calculations at DLPNO-CCSD(T).[52,59]

The solvation effects have been considered by re-optimizing and characterizing all stationary points employing the M06-2X functional using a polarizable implicit solvent model (PCM)[60] with water as solvent, where the solvation free energies have been calculated taken into account the conversion between the gas phase standard state at 298 K and 1 atm to 1 M reference state in solvation (see ESI†). The role of explicit water molecules has also been discussed using a combined implicit–explicit model.

For the reactions involving compounds **1**, **2**, and **3** with HO_2 radical, the rate constants have been calculated according to conventional transition state theory taking into account tunneling effects for an unsymmetrical Eckart barrier.[61] For reactions with compound **4** with HO_2 radical, the kinetics calculations have been computed according to conventional transition state theory, but in the framework of multi-conformer transition state theory (MC-TST). In this case we have taken into account the tunneling effects according to the Wigner approach The reactions of sulfenic acids with OH radical are predicted to be diffusion controlled, and we have computed the association rate constants of **1**, **2**, and **3** with OH radical employing the VRC-VTST (variable reaction coordinate – variational transition state theory).[62,63] Further details of theoretical approaches used are described in the ESI.†

Results and discussion

All reactions investigated begin with the formation of a pre-reactive complex between the corresponding sulfenic acid and the hydroxyl or hydroperoxyl radical. The reactions continue through a transition state and lead to the formation of a post-reactive complex before the release of the products. We have named every stationary point by a number, which identifies the compound as in Scheme 1, followed for the letter A or B, identifying that the reaction takes place with HO_2 of HO radicals respectively, followed by the letters R for reactant, CR for pre-reactive complex TS for transition states, or CP for post-reactive complex, and followed by a number. Thus, for instance, **1ATS2** identifies the transition state number 2 for the reaction of compound **1** (CH_3SOH) with HO_2, while **3BCR1** identifies the pre-reactive complex number 1 of the reaction of compound **3** ($CH_3CHCHSOH$) with OH.

We will begin analyzing some properties of the **1–4** sulfenic acids, and continue by discussing the reaction mechanisms. First, we will pay attention to the reaction of the parent methane–sulfenic acid (**1**) with hydroperoxyl and hydroxyl radicals, and will discuss the main electronic features. We will continue analyzing the reactivity of compounds **2**, **3**, and **4**. Finally, we will discuss the effects of water solvation, and we will report the computed rate constants.

In a previous work, we investigated the reactivity of hydropersulfide (CH_3SSH) with hydroxyl radical,[64] showing that there is a competence between the addition of the radical to one of the sulfur atoms and the abstraction of the acidic hydrogen atom. Because CH_3SSH and CH_3SOH have the same number of valence electrons, we have also considered both possibilities for the reaction of sulfenic acids with OH and HO_2 radical. In addition, we have also considered the possible abstraction of one hydrogen atom of the methyl group for the reaction of **1** + OH and the addition of the OH radical to the π bonds in the reactions of **2** and **3** with OH.

A. The sulfenic acids 1–4

Little is known about the acidity of sulfenic aids, and the few available values in the literature cover a wide range of pK_a, from 4.8 for lumazine–sulfenic acid and 6.3 for 1-methyluracil-4-sulfenic acid,[36] to 12.5 for triptycenyl sulfenic acid[65] and 10.47 for 2-methyl-2-propanesulfenic acid.[66] Therefore, we have first calculated the gas phase acidity and estimated the corresponding pK_a in water. The pK_a values have been calculated by considering the thermodynamic cycle reported in the ESI.† Absolute pK_a values are obtained by taking the experimental pK_a of 2-methyl-2-propanesulfenic acid, $(CH_3)_3SOH$, as the reference, and calculating relative δpK_a values from the process R-SOH + $(CH_3)_3$-SO^- → R-SO^- + $(CH_3)_3$-SOH. Our results are displayed in Table 1. Note that our computed gas phase acidity of compound **1** compares very well with the experimental value. The estimated pK_a values of compounds **1–4** range between 8.4 and 11.3 implying that all these species will be in an unionized form aqueous environments, such as in atmospheric clouds or in biological conditions, and that therefore they can react with OH and HO_2 radicals.

B. Reaction of sulfenic acid compounds with HO_2 radical

Our results, presented in Fig. 1–3 and Table 1, provide new insights into the reaction of methane sulfenic acid with HO_2,

Table 1 Calculated gas phase acidity (in kcal mol^{-1}), free energies of solvation (in kcal mol^{-1}) and pK_a values for sulfenic acids[a]

	$\Delta G_{acidity}$[b] (gas phase)				
Compound	Calculated	Exp.[c]	ΔG_{solv} (RSOH)	ΔG_{solv} (RSO^-)	pK_a
$(CH_3)_3SOH$	349.0	—	−3.7	−61.5	10.47[d]
1	352.5	352.0 ± 3.0	−4.0	−66.1	9.90[e]
2	349.0	—	−3.7	−63.8	8.88[e]
3	345.7	—	−4.1	−61.4	8.46[e]
4	334.6	—	−12.2	−54.5	11.30[e]

[a] Calculated taking the CCSD(T) energies (DLPNO-CCSD(T) in the case of compound 4) and free energy corrections at M06-2X level. [b] Corresponds to the R-SOH → RSO^- + H^+ reaction. [c] Taken from ref. 67. [d] Experimental value from ref. 66. [e] Calculated by adding to the experimental values the δpK_a according the R-SOH + $(CH_3)_3$-SO^- ⇌ R-SO^- + $(CH_3)_3$-SOH equilibrium.

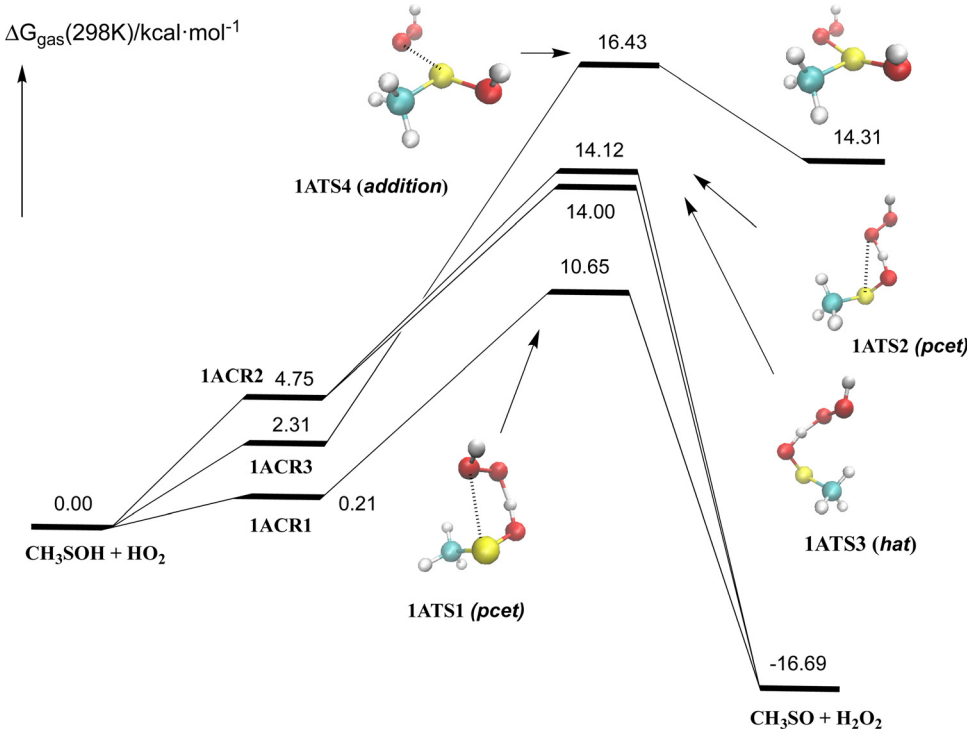

Fig. 1 Schematic free energy surface for the reaction of methane sulfenic acid CH_3SOH with HO_2, computed at CCSD(T)/aug-cc-pV(T+d)Z level of theory with free energy corrections obtained at M06-2X level.

complementing previous studies on sulfenic acids reacting with HO_2 and methoxy radicals reported in the literature.[28–31,68] Fig. 1 illustrates the free energy profile of the gas-phase reaction of methane sulfenic acid with HO_2, offering a representation of the reaction pathway. Fig. 2 highlights the most relevant electronic features of the processes involved, revealing details that enhance our understanding of the reaction mechanisms. Further data can be found in Table 1 and the ESI.†

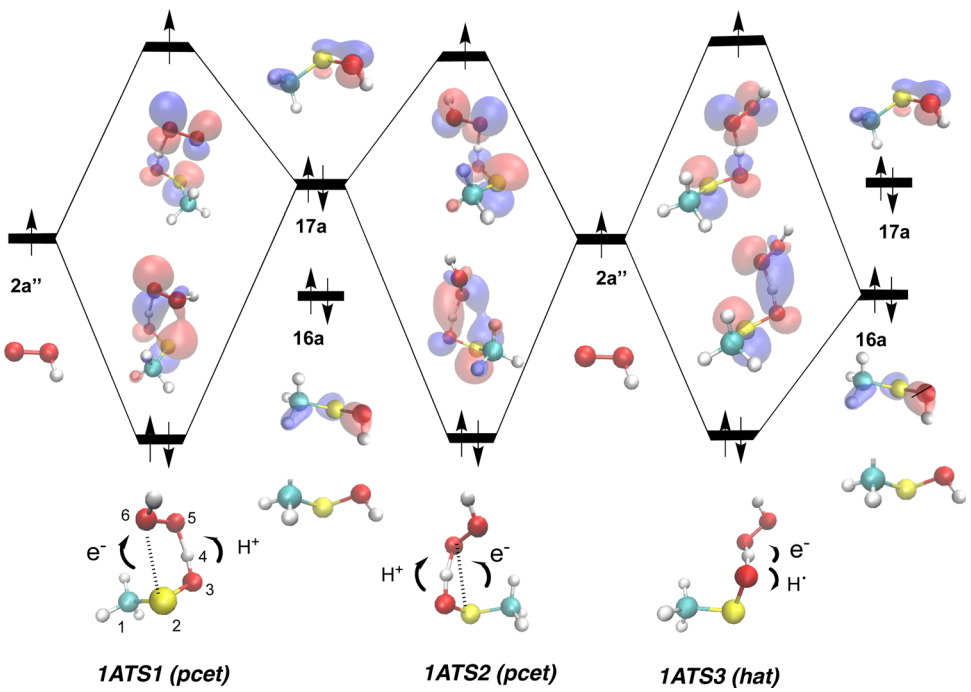

Fig. 2 Electronic features for the different elementary reaction of the hydrogen abstraction of CH_3SOH by HO_2.

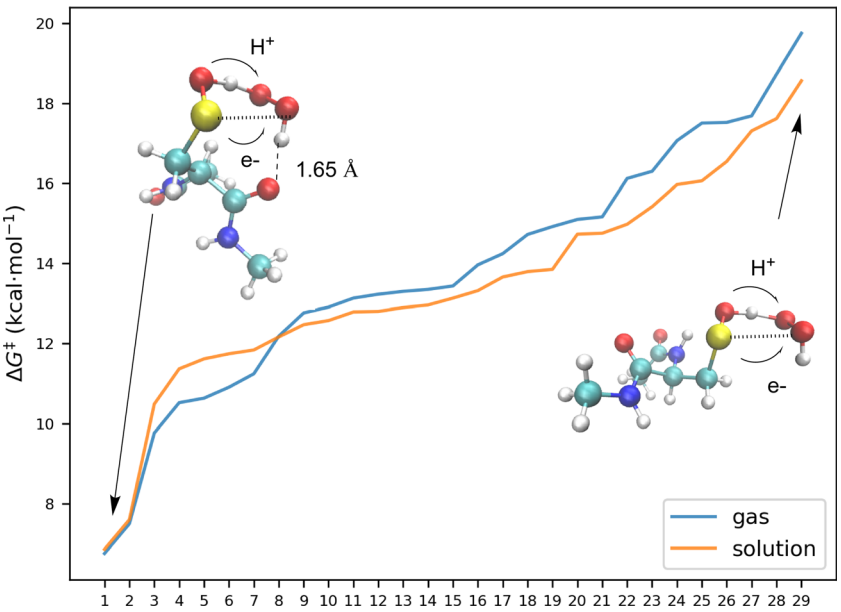

Fig. 3 Relative free energy differences at 298 K between the different conformers of the transition states with the lowest reactant **4**. Each elementary reaction involves the acidic hydrogen abstraction by HO_2 following the pcet mechanism with the same electronic features as described for **1ATS1** above. The free energies are computed at DLPNO-CCSD(T)/aug-cc-pVTZ level of theory, with free energy corrections obtained at M06-2X level, and corrected by −3.8 kcal mol^{-1}. See (ESI†).

We have found three different kinds of processes for the abstraction of the hydrogen acid by the radical, with free energy barriers at 298 K of 10.65, 12.00, and 14.12 kcal mol^{-1} (*via* **1ATS1**, **1ATS2**, and **1ATS3**, respectively), all of them leading to the formation of methylsulfinyl radical (CH_3SO) radical[69] and H_2O_2. The reaction is calculated to be exoergic by 16.69 kcal mol^{-1}. We have also found an additional reaction path involving the addition of the HO_2 radical to the sulfur atom (*via* **1ATS4**) with a computed energy barrier of 16.43 kcal mol^{-1}, producing the $CH_3S(OH)_2$ radical which is endoergic by 14.31 kcal mol^{-1}. Further work (not displayed in Fig. 1) has shown that the $CH_3S(OH)_2$ radical easily hydrolyzes to CH_3SO + H_2O_2 + H_2O (see the ESI†).

Table 2 Relative energies ($\Delta(E + ZPE)_{gas}$), free energies at gas and aqueous phases (ΔG_{gas} and ΔG_{sol}) at 298 K, and computed rate constants (in M^{-1} s^{-1}) at 298 K

	$\Delta(E + ZPE)_{gas}$	ΔG_{gas}	ΔG_{sol}	k_{gas}[d]	k_{solv}
RSOH + HO_2 → RSO + H_2O_2					
1ATS1[a]	0.17	10.65	11.35	3.84×10^{6} (6.38×10^{-15})	8.74×10^{4}
2ATS1[a]	−0.45	10.11	11.19	1.39×10^{7} (2.31×10^{-14})	2.14×10^{5}
3ATS1[a]	0.37	10.98	11.62	2.12×10^{6} (3.52×10^{-15})	6.87×10^{4}
4ATS1[b,c]	−4.33	6.76	6.86	1.15×10^{8} (7.37×10^{-15})	5.37×10^{7}

	$\Delta(E + ZPE)_{gas}$	ΔG_{gas}	ΔG_{sol}	k_{gas}[d]
RSOH + OH → RSO + H_2O				
1BTS1[a]	−14.27	−5.41	−5.51	Diffusion controled (6.31×10^{-10})[e]
2BTS1[b]	−16.75	−7.71	−6.87	Diffusion controled (2.51×10^{-9})[e,f]
3BTS1[b]	−15.71	−6.92	−7.61	Diffusion controled (7.96×10^{-10})[e]
4BTS1[b,c]	−14.33	−5.63	−4.49	Diffusion controled

[a] Computed at CCSD(T)/aug-cc-pV(T+d)Z level, with zero point energy and free energy corrections obtained at M06-2X level. [b] Computed at DLPNO-CCSD(T)/(aug-cc-p)Z level, with zero point energy and free energy corrections obtained at M06-2X level. The corresponding values are corrected by −3.8 kcal mol^{-1}. See ESI. [c] Relative energy between the reactant having the lowest free energy and the transition state with the lowest energy. [d] Gas phase rate constants are given in M^{-1} s^{-1} to allow comparison with solvation. The values in cm^3 molecule^{-1} s^{-1} are given in parenthesis. [e] Gas phase rate constant computed at VRC-VTST level of theory. [f] Rate constant of VRC-VTST association reaction of three pre-reactive complexes (**2BCR1** = 7.37×10^{-10} cm^3 molecule^{-1} s^{-1}, **2BCR1a** = 1.2×10^{-9} cm^3 molecule^{-1} s^{-1} and **2BCR1b** = 6.48×10^{-10} cm^3 molecule^{-1} s^{-1}, see ESI).

The analysis of the electronic structure, displayed in Fig. 2, shows that **1ATS1** and **1ATS2** follow a proton coupled electron transfer (pcet) mechanism and **1ATS3** involves a conventional hydrogen atom transfer mechanism (hat).

1ATS1 has the same electronic features described for the reaction of HSOH + HO_2 and the reaction of sulfenic acids with methoxy and alkoxy radical,[28–30] and involves the transfer of one electron from the sulfur atom 2 to the oxygen atom 6 and simultaneously the jump of the proton 4 to the oxygen atom 7 (see Fig. 2 for atom numbering). On the other side, in **1ATS2** the electron is transferred from the sulfur atom 2 to the oxygen atom 5 and the proton is transferred to the same oxygen atom. Please note that the distance of the atoms with which the electron is transferred is much larger in **1ATS2** (3.01 Å) than in **1ATS1** (2.83 Å), having the latter a smaller free energy barrier by 3.6 kcal mol^{-1} (see ESI† for more details). The elementary reaction through **1ATS3** (hat mechanism) occurs by the simultaneous breaking and forming of the (RS)O–H and H–(OOH) bonds requiring a much higher energy barrier than in **1ATS1**.

Substitution of the $–CH_3$ by $–CH_2–CH{=}CH_2$ and $–CH{=}CH–CH_3$ groups (compounds **2** and **3**) in the reaction with HO_2 does not lead to significant differences, neither in the reaction mechanisms nor in the corresponding energy barriers. Table 2 shows that the reaction free energy of the lowest reaction path differ in these cases by tens of kcal mol^{-1}, and the free energy barrier compare very well with that reported in the literature.[31] The addition of the radical to the sulfur atom lies higher in energy and differs by less than 1 kcal mol^{-1} compared with the reaction of CH_3SOH, and is described in the ESI.†

The results for the reaction of the model **4** with HO_2, are summarized in Fig. 3, which collects the relative free energy barrier of the different conformers of the transition states with respect to the free energies of the most stable R-SOH + HO_2 reactants. The figure shows differences up to 11 kcal mol^{-1} in the energy barrier of the hydrogen abstraction process along the different compounds studied. Our results show that the free energy barrier of the most favorable path is computed to be about 4 kcal mol^{-1} smaller than in the reaction of compounds **1**, **2**, and **3** with HO_2 (see Table 2). A detailed analysis of the different transition states indicates that in all cases considered, the processes have the same electronic features as described for **1ATS1** above, and the differences in the energy barriers may be associated to side interactions. In Fig. 3 we have also included the structures of the transition states of the reaction paths with the lowest and highest energy barrier (**4ATS1_1**, and **4ATS1-33**, numbers 1 and 29 in Fig. 3). Fig. 3 shows that the **4ATS1_1** is stabilized by a strong hydrogen bond (d(H–O) = 1.65 Å) between the terminal hydrogen atom of the hydroperoxyl moiety and one oxygen atom of the carbonyl group, which does not exist in **4ATS1_33**, and these results clearly highlight the importance of further interactions on the energy barriers of these processes. Again, other elementary reactions, such as the addition of the radical to the S atom, do not have any impact in the reaction rate and are discussed in the ESI.†

C. Reaction of sulfenic acid compounds with OH radical

Fig. 4 contains a schematic potential free energy surface for the reaction of methane sulfenic acid with hydroxyl radical. Again, and as mentioned above, each elementary reaction begins with the formation of a pre-reactive complex before the transition state and the release of the products.

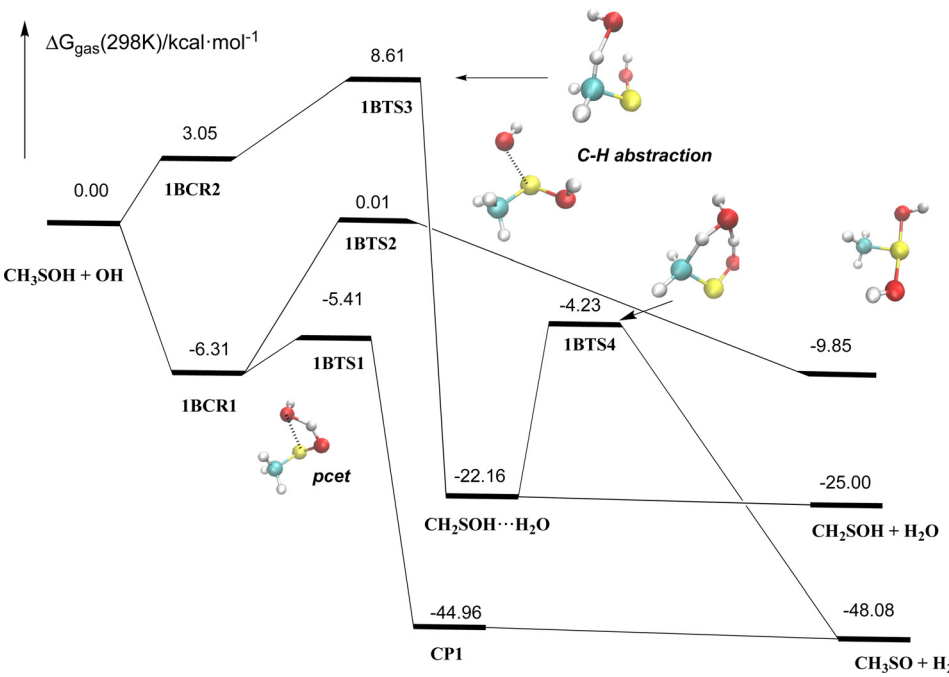

Fig. 4 Schematic free energy surface for the reaction of methane sulfenic acid CH_3SOH with OH, computed at CCSD(T)/aug-cc-pV(T+d)Z level of theory with free energy corrections obtained at M06-2X level.

As pointed out above, we have considered three different elementary reactions, namely the abstraction of the acidic hydrogen by the OH radical (*via* **1BTS1**), the addition of the radical to sulfur atom (*via* **1BTS2**), and the abstraction of one hydrogen atom of the methyl group (*via* **1BTS3**). Our results show that the two first elementary processes begin with the **1BCR1** pre-reactive complex, and the free energy of the transition state for the hydrogen abstraction by the OH radical (**1BTS1**) lies below the free energy of the reactants (−5.41 kcal mol^{-1}), which means that the reaction is controlled by diffusion, in contrast with the reaction of CH_3SOH with HO_2 described above, and any encounter between methane sulfenic acid and hydroxyl radical will produce the CH_3SO radical and H_2O. We predict this reaction to be exoergic by 48.08 kcal mol^{-1}. Fig. 4 shows that the free energy barrier fort the addition of the OH radical to CH_3SOH (*via* **1BTS2**) is isoergonic with respect to the separate reactants, producing $CH_3S(OH)_2$, which, although not shown in Fig. 4, easily hydrolyzes producing $CH_3SO + 2H_2O$ (see the ESI†). Finally, the abstraction of one hydrogen atom of the methyl group by the OH radical (*via* **1BTS3**) requires a much higher free energy barrier (8.61 kcal mol^{-1}), producing either $CH_2SOH + H_2O$ or through a double proton transfer (*via* **1BTS4**) leading to $CH_3SO + H_2O$. Because the abstraction of the acidic hydrogen atom by OH is predicted to be diffusion controlled, we can conclude that the abstraction of the hydrogen atom of the methyl group will not occur.

Fig. 5(a) shows that the abstraction of the acidic hydrogen atom (**1BTS1**) follows a pcet mechanism, which is characterized by a system of three electrons in two orbitals and involve the transfer of one electron from the sulfur atom 2 to the oxygen atom (5) of the radical and the simultaneous transfer for the proton 4 from the oxygen of the CH_3SOH to the oxygen of the radical. This kind of pcet processes described by a system of three electrons in two orbitals has been already described for other kind of reactions.[64,70–74]

It is also worth comparing the reactions of sulfenic acid and hydropersulfide (CH_3SSH) with hydroxyl radical. Both compounds show great similarities as they have the same number of valence electrons and behave as good antioxidants with great ability to scavenge radicals.[75,76] Moreover, RSSH can be also a precursor of sulfenic acids by reacting with OH radicals.[64] In the case of the oxidation of CH_3SSH with OH, results from the literature indicate that there is a competition between the addition of the radical to one sulfur atom and the hydrogen abstraction, the latter, taking place *via* a pcet mechanism.[64] For the purposes of the present work, we have compared the H abstraction process in both reactions. Fig. 5(a) and (b) reveal that both reactions follow a pcet mechanism, having the same electronic features at the transition states as described above. However, there are significant differences in their energetics. Whereas the reaction of OH with RSSH needs to surmount a free energy barrier of 6.41 kcal mol^{-1} with respect to the reactants, the substitution of SH by OH in CH_3SOH results in a drop of the relative free energy of the transition state by 11.8 kcal mol^{-1} so that the reaction becomes diffusion controlled as discussed above. The differences in these energy

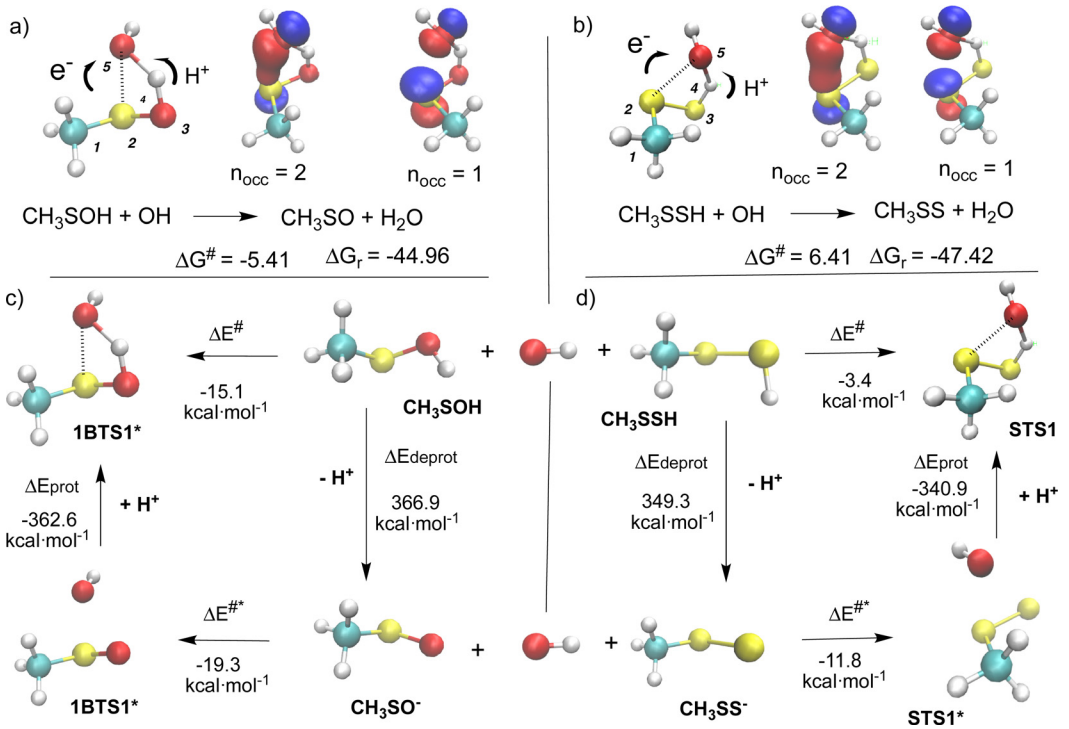

Fig. 5 Electronic features of the pcet mechanisms of the reactions between CH_3SOH and CH_3SSH with OH and the thermodynamic cycles comparing the deprotonation of the CH_3SOH and CH_3SSH reactants with those of the transition states and the energetic requirements for the formation of these structures. The energies are computed at CCSD(T)/aug-cc-pV(T+d)Z level of theory with free energy corrections obtained at M06-2X level.

barriers can be rationalized considering a thermodynamic cycle following Mayer and co-workers[77] and also applied in ref. 72. As described in Fig. 5(c) and (d), the first step correspond to the deprotonation energy of the reactants, which requires more energy for the CH_3SOH compared with CH_3SSH (17.6 kcal mol^{-1}). The second step consist in bringing the anions and the hydroxyl radical to the structure of the transition state without the proton (**1BTS1*** and **STS1***), which is more favorable in the case of sulfenic acid by 7.5 kca mol^{-1}, and the third step consist in calculating the energy liberated in bringing the proton to the structure of the transition state (**1BTS1** and **STS1**), favorable by 21.7 kcal mol^{-1} for the sulfenic acid with hydroxyl radical process, so that the formation of **1BTS1** is more favorable by 11.7 kcal mol^{-1} than the formation of **STS1**.

The potential impact of these reactions in the chemistry of the atmosphere deserves some comments. In one hand, for the $CH_3SOH + HO_2$ reaction, our calculations predict a rate constant of 6.38×10^{-15} cm^3 $molecule^{-1}$ s^{-1}, at 298 K, and an Arrhenius equation $k = 4.45 \times 10^{-15} e^{\left(\frac{0.21}{RT}\right)}$ in the range of 200–320 K temperatures. Although the atmospheric concentration of HO_2 is about two orders of magnitude greater than that of OH,[1] the reaction of sulfenic acid with HO_2 cannot compete with the reaction with OH, which is predicted to be diffusion controlled. Table 2, Fig. 4 and Table S2 (ESI†) show that the free energy at 298 K of **1BTS1** lies 5.41 kcal mol^{-1} below the free energy of the separate reactants and therefore the rate constant depends on the association between CH_3SOH and OH. Calculations at VRC-VTST[62] predict a rate constant of 6.31×10^{-10} cm^3 $molecule^{-1}$ s^{-1} (see Table 2).

On the other hand, recent work has shown that in the troposphere, methane sulfenic acid reacts with ozone, with a reported rate constant of 2×10^{-12} cm^3 $molecule^{-1}$ s^{-1}.[20] It is therefore expected that this reaction is the major cause of atmospheric CH_3SOH oxidation in ozone polluted areas, where the atmospheric concentration of ozone may be 5 to 7 orders of magnitude greater that the concentration of hydroxyl radical. However, in O_3 free atmospheres, where the OH radical is formed by photolysis of HONO,[78] the reaction of methane sulfenic acid with hydroxyl radical should play the major role.

The reaction of compounds **2**, **3**, and **4** with OH follows the same trends as for the reaction of compound **1**. In all cases, the hydrogen abstraction by the radical involves a pcet mechanism, and we have found three different elementary reactions for the reaction between 2 and OH and one elementary reaction for the reaction between 3 and OH (see Table 2 and Tables S5, S6 of the ESI†). In all these processes, the free energy barrier lies below the free energy of the reactants indicating that all these reactions are diffusion controlled. For reactions of **2** and **3** with OH radical we have also calculated the association rate constant at VRC-VTST level of theory and the computed values are 2.51×10^{-9} and 7.96×10^{-10} cm^3 $molecule^{-1}$ s^{-1}, respectively (see Table 2).

Beyond the acidic hydrogen abstraction by the hydroxyl radical, we have also considered the addition of the radical to the S atom of the sulfenic acid and for the reactions of **2** and **3** with OH the addition of the radical to the π bond. In all these cases, these processes require to surmount a free energy barrier and therefore are expected not to occur (see Tables S3–S6 of the ESI†).

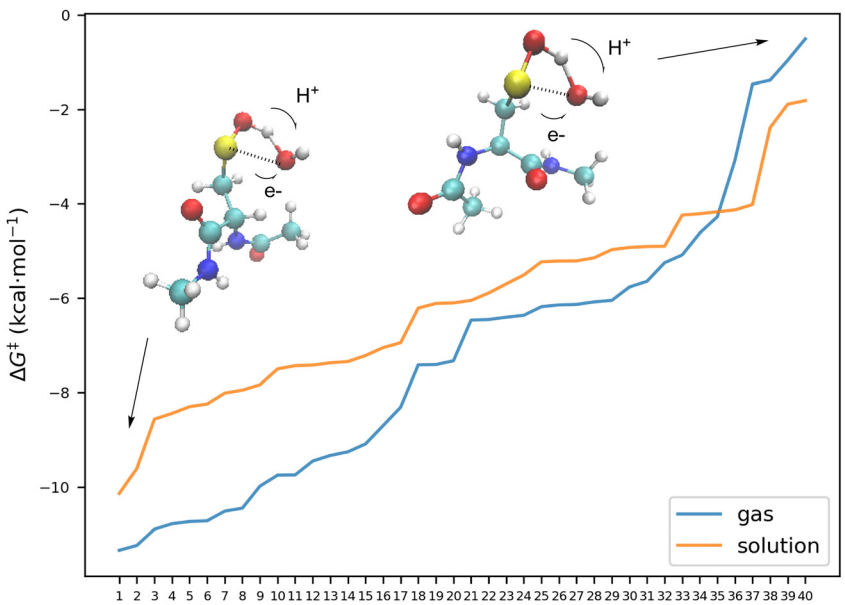

Fig. 6 Free energy barriers at 298 K of the different conformers of the transition states relative to their reactants for the reaction of **4** with OH. Each elementary reaction involves the acidic hydrogen abstraction by OH following the pcet mechanism with the same electronic features as described for **1BTS1** above. The free energies are computed at DLPNO-CCSD(T)/aug-cc-pVTZ level of theory, with free energy corrections obtained at M06-2X level, and corrected by −3.8 kcal mol^{-1}. See the (ESI†).

In Fig. 6 we have collected the free energy barriers of all elementary reactions involving the abstraction of the acidic hydrogen of the sulfenic acid by the hydroxyl radical, along the structures of the transition state of the elementary reaction having the smaller and larger energy barrier. In line with the reaction of **4** with HO_2 discussed above, we have found differences up to 10.83 kcal mol^{-1} in the energy barriers which depend on the interaction of the reacting group with other groups. Thus, in the transition state with the highest energy barrier, there is a repulsive interaction between the oxygen atom of the radical moiety and one nitrogen atom of the peptide bond which makes this stationary point less stable.

D. Aqueous environments

The kinetics of the oxidation reactions described above in the gas phase involving sulfenic acids and HO_x radicals may change when the processes take place in aqueous environments, such as aqueous aerosols in the atmosphere, surface waters (rivers, lakes, *etc.*) or biological systems. To estimate the importance of solvent effects in such conditions, we have made systematic calculations for these processes in water solution using the PCM implicit solvent model. All structures have been reoptimized in solution and the free energies have been calculated according to the methodology described in the computational section.

As shown in Table 1 and Fig. 3, 6, the inclusion of solvent effects through the PCM model modifies the activation free energies of the different mechanisms and systems, but the changes are small. Again, the most favorable reaction involves the abstraction of the acidic hydrogen by the radical, *via* a pcet mechanism. The values in Table 1, which summarizes the activation free energies, illustrate the main trends. In the case of the reactions in aqueous solution with HO_2, the barriers are slightly higher compared to gas phase values, with the largest difference amounting about 0.7 kcal mol^{-1}, in line with the data reported for the reaction of **2** with HO_2.[31] Again, the free energy barriers for compounds **1–3** are very close to each other, but it is smaller by about 3.5 kcal mol^{-1} for compound **4** in the same way as discussed for the gas phase.

In the case of the reactions with OH, which all display negative energy barriers, with differences in the free energy barrier smaller than 1.0 kcal mol^{-1} compared to the gas phase, all abstraction reactions are expected to be diffusion controlled.

Overall, Table 1 shows that our calculated rate constants obtained for the reaction between compounds **1–3** with HO_2, using a continuum solvent model are between 31 and 65 times smaller than in gas phase, and range between 6.87×10^4 and 2.15×10^5 M^{-1} s^{-1}, compared with the 2.60×10^7 M^{-1} s^{-1} reported for the **2** + HO_2.[31] For the reaction between compound **4** with HO_2, the computed rate constant in solvation is just 2.14 times smaller than that in gas phase, and the reaction is predicted to be much faster than for compounds **1–3**, with a computed rate constant of 5.37×10^7 M^{-1} s^{-1} in liquid phase.

Nevertheless, the reactive systems contain several polar bonds that are likely to exhibit specific solute–solvent interactions such as hydrogen-bonds, and these interactions bring an additional stabilizing contribution to the solvation energies of the structures. The effect of solute–solvent hydrogen-bond formation with the reactants and the transition state was examined before in the case of the reaction **2** + HO_2 using a similar quantum level as the one used in ref. 31. The authors used a discrete-continuum solvation model in which one explicit water molecule is included in the calculations, and the PCM model is used to account for the interactions with the dielectric continuum. They reported a barrier of 11.65 kcal mol^{-1}, which is close to the value obtained with a pure PCM model (10.17 kcal mol^{-1}). In order to see if this effect could be extended to our systems, we have also carried out a similar calculation on the most stable conformer of the reaction between **4** and HO_2, and our results indicate that using a discrete-continuum solvation model with one explicit water molecule, the free energy barrier increases by 1.5 kcal mol^{-1} compared to the calculations with a pure PCM model in a similar way as reported for **2** + HO_2, (see the ESI† for more details), and therefore we conclude that this effect is small.

In addition, as the reactions studied involve the transfer of H atoms carrying a varying degree of positive charge, it is also conceivable that water molecules actively assist the processes by participating to the reaction coordinate as proton relays. In order to take into account this possibility we have looked for processes where one water molecule acts as an intermediate in the proton transfer, namely one electron is transferred from the S atom to the terminal O atom of OH or HO_2, whereas the acidic proton of the sulfenic acid is transferred to the water molecule and simultaneously, one proton from water is transferred to the OH or HO_2 moiety. Our results are detailed in the ESI† and predict that the reactions with HO_2 radicals require higher energy barriers, so that this mechanism should not be operative. For the reaction with OH, all transition states still have a negative energy barrier, and consequently, the reactions remain diffusion controlled.

The high reactivity of sulfenic acids with hydroxyl radical in different environments suggests a strong antioxidant ability of these species, in line with the antioxidant capacity of disulfide compounds, whose reaction with OH radicals[41] contributes to the defense of biological systems against ROS species. Besides, one may note that one of the products of the reactions investigated are sulfinyl radicals (R-SO), which are less reactive than HO_x, thiyl and perthiyl radicals, and have interest in environmental, organic and biochemical chemistry.[11,79–83] Finally, it must be emphasized that in aqueous environments, the reaction of sulfenic acids with hydroperoxyl radical, whose pK_a is 4.8, will have relevance in acidic media.

Conclusions

In summary, we explored the structure–function relationship for a series of sulfenic acids reacting with OH and HO_2 in both gas phase and aqueous environments. We identified two main mechanisms: hydrogen abstraction (hat) and proton-coupled electron transfer (pcet), and our findings indicate that pcet predominates.

The reactions with either OH or HO_2 can proceed *via* two pathways: addition or abstraction. For the CH_3SOH (**1**) + HO_2 reaction, the two pathways lead to the same product, which is consistent with the existing literature, and favors H_2O_2 production, which has significant biochemical implications. For the CH_3SOH (**1**) + OH reaction, the major products are CH_3SO (H abstraction) and $CH_3S(OH)_2$ (OH addition), with the latter compound easily hydrolyzing to CH_3SO and water. Abstraction of the hydrogen from the methyl group of CH_3SOH will not occur; this step was found to have the largest activation energy among the collective steps in the mechanism. The CH_3SOH + OH_x reaction has relevance in the atmosphere and we predict a rate constant of 6.38×10^{-15} cm^3 $molecule^{-1}$ s^{-1} at 298 K for the reaction with HO_2 and diffusion control for the reaction with OH, implying that the latter will be the most important oxidation process of CH_3SOH in ozone free atmosphere.

An important finding is that the reactions of all sulfenic acids with hydroxyl radical are diffusion controlled, even when a water molecule participates as reactant in the whole process. Their rate constants depend on the association process between the sulfenic acid and the hydroxyl radical, and have been calculated to be 6.31×10^{-10}, 2.51×10^{-9}, and 7.96×10^{-10} cm^3 $molecule^{-1}$ s^{-1}, for the gas phase reactions of **1**, **2**, and **3** with OH respectively. Our results suggest that in O_3 free atmospheres, where the OH radical is formed by photolysis of HONO, the reaction of methane sulfenic acid with hydroxyl radical should play the major role.

For the reaction of **2**, and **3** with HO_2, our calculations predict rate constants 6.87×10^4 and 2.14×10^5 M^{-1} s^{-1}, which is not very different from the rate constant for compound **1**, but a much larger value is obtained for the reaction of the model system **4** with HO_2 (5.37×10^7 M^{-1} s^{-1}). In the last case, the interaction of the reacting group with the peptide bond patterns in the molecule produces a significant stabilization effect of the transition state that can be translated to the reaction of sulfenic acids in proteins. The very high reactivity of sulfenic acids with the hydroxyl radical suggests a strong antioxidant capacity of these species.

Data availability

The data supporting the findings of this study are available within the article and its ESI.†

Conflicts of interest

There are no conflicts to declare.

Acknowledgements

JMA and RC thank the Spanish Ministerio de Ciencia e Inovación (grant PID2022-138040OB-I00) for financial support, and the Consorci de Serveis Universitaris de Catalunya (CSUC) and the Centro de Supercomputación de. Galicia (CESGA) for providing computational resources.

References

1 Paul S. Monks, *Chem. Soc. Rev.*, 2005, **34**, 376–395.
2 J. M. Anglada, M. Martins-Costa, J. S. Francisco and M. F. Ruiz-Lopez, *Acc. Chem. Res.*, 2015, **48**, 575–583.
3 S. Parvez, M. J. C. Long, J. R. Poganik and Y. Aye, *Chem. Rev.*, 2018, **118**, 8798–8888.
4 B. Halliwell, *Plant Physiol.*, 2006, **141**, 312–322.
5 M. Iriti and F. Faoro, *Water, Air, Soil Pollut.*, 2008, **187**, 285–301.
6 O. Sorg, *C. R. Biol.*, 2004, **327**, 649–662.
7 G. Xu and M. R. Chance, *Chem. Rev.*, 2007, **107**, 3514–3543.
8 K. U. Ingold and D. A. Pratt, *Chem. Rev.*, 2014, **114**, 9022–9046.
9 E. Block, *Angew. Chem., Int. Ed. Engl.*, 1992, **31**, 1135–1178.
10 E. Block, *Reactions of Organosulfur Compounds: Organic Chemistry: A Series of Monographs*, Academic Press, 2013, vol. 37.
11 I. Barnes, J. Hjorth and N. Mihalopoulos, *Chem. Rev.*, 2006, **106**, 940–975.
12 S. Meinardi, I. J. Simpson, N. J. Blake, D. R. Blake and F. S. Rowland, *Geophys. Res. Lett.*, 2003, **30**, 1454.
13 G. A. Novak, D. B. Kilgour, C. M. Jernigan, M. P. Vermeuel and T. H. Bertram, *Atmos. Chem. Phys.*, 2022, **22**, 6309–6325.
14 J. Zhao, G. Sarwar, B. Gantt, K. Foley, B. H. Henderson, H. O. T. Pye, K. M. Fahey, D. Kang, R. Mathur, Y. Zhang, Q. Li and A. Saiz-Lopez, *Atmos. Environ.*, 2021, **244**, 117961.
15 S. Li, G. Sarwar, J. Zhao, Y. Zhang, S. Zhou, Y. Chen, G. Yang and A. Saiz-Lopez, *Earth Space Sci.*, 2020, **7**, e2020EA001220.
16 J. Shen, W. Scholz, X.-C. He, P. Zhou, G. Marie, M. Wang, R. Marten, M. Surdu, B. Rörup, R. Baalbaki, A. Amorim, F. Ataei, D. M. Bell, B. Bertozzi, Z. Brasseur, L. Caudillo, D. Chen, B. Chu, L. Dada, J. Duplissy, H. Finkenzeller, M. Granzin, R. Guida, M. Heinritzi, V. Hofbauer, S. Iyer, D. Kemppainen, W. Kong, J. E. Krechmer, A. Kürten, H. Lamkaddam, C. P. Lee, B. Lopez, N. G. A. Mahfouz, H. E. Manninen, D. Massabò, R. L. Mauldin, B. Mentler, T. Müller, J. Pfeifer, M. Philippov, A. A. Piedehierro, P. Roldin, S. Schobesberger, M. Simon, D. Stolzenburg, Y. J. Tham, A. Tomé, N. S. Umo, D. Wang, Y. Wang, S. K. Weber, A. Welti, R. Wollesen de Jonge, Y. Wu, M. Zauner-Wieczorek, F. Zust, U. Baltensperger, J. Curtius, R. C. Flagan, A. Hansel, O. Möhler, T. Petäjä, R. Volkamer, M. Kulmala, K. Lehtipalo, M. Rissanen, J. Kirkby, I. El-Haddad, F. Bianchi, M. Sipilä, N. M. Donahue and D. R. Worsnop, *Environ. Sci. Technol.*, 2022, **56**, 13931–13944.
17 J. Chen, J. R. Lane, K. H. Bates and H. G. Kjaergaard, *Environ. Sci. Technol.*, 2023, **57**, 21168–21177.
18 S. Hatakeyama and H. Akimoto, *J. Phys. Chem.*, 1983, **87**, 2387–2395.
19 I. Barnes, K. H. Becker and N. Mihalopoulos, *J. Atmos. Chem.*, 1994, **18**, 267–289.
20 T. Berndt, J. Chen, K. H. Møller, N. Hyttinen, N. L. Prisle, A. Tilgner, E. H. Hoffmann, H. Herrmann and H. G. Kjaergaard, *Chem. Commun.*, 2020, **56**, 13634–13637.
21 S. Lacombe, M. Loudet, E. Banchereau, M. Simon and G. Pfister-Guillouzo, *J. Am. Chem. Soc.*, 1996, **118**, 1131–1138.
22 R. E. Penn, E. Block and L. K. Revelle, *J. Am. Chem. Soc.*, 1978, **100**, 3622–3623.

23 X. Shao, J. Xue, J. Jiang and X. Zeng, *J. Phys. Chem. Lett.*, 2024, **15**, 7327–7334.
24 C. Jacob, *Nat. Prod. Rep.*, 2006, **23**, 851–863.
25 A. N. Jikah and G. I. Edo, *Pharmacol. Res. – Mod. Chin. Med.*, 2023, **9**, 100323.
26 R. Kubec, R. B. Cody, A. J. Dane, R. A. Musah, J. Schraml, A. Vattekkatte and E. Block, *J. Agric. Food Chem.*, 2010, **58**, 1121–1128.
27 Y. Okada, K. Tanaka, I. Fujita, E. Sato and H. Okajima, *Redox Rep.*, 2005, **10**, 96–102.
28 P. T. Lynett, K. Butts, V. Vaidya, G. E. Garrett and D. A. Pratt, *Org. Biomol. Chem.*, 2011, **9**, 3320–3330.
29 R. Amorati, P. T. Lynett, L. Valgimigli and D. A. Pratt, *Chem. – Eur. J.*, 2012, **18**, 6370–6379.
30 V. Vaidya, K. U. Ingold and D. A. Pratt, *Angew. Chem., Int. Ed.*, 2009, **48**, 157–160.
31 A. Galano and M. Francisco-Marquez, *J. Phys. Chem. B*, 2009, **113**, 16077–16081.
32 K. Seki, J. Ishikawa and Y. Okada, *J. Food Sci.*, 2018, **83**, 1265–1270.
33 J. M. Fukuto, L. J. Ignarro, P. Nagy, D. A. Wink, C. G. Kevil, M. Feelisch, M. M. Cortese-Krott, C. L. Bianco, Y. Kumagai, A. J. Hobbs, J. Lin, T. Ida and T. Akaike, *FEBS Lett.*, 2018, **592**, 2140–2152.
34 D. Garrido Ruiz, A. Sandoval-Perez, A. V. Rangarajan, E. L. Gunderson and M. P. Jacobson, *Biochemistry*, 2022, **61**, 2165–2176.
35 L. B. Poole, P. A. Karplus and A. Claiborne, *Annu. Rev. Pharmacol. Toxicol.*, 2004, **44**, 325–347.
36 V. Gupta and K. S. Carroll, *Biochim. Biophys. Acta*, 2014, **1840**, 847–875.
37 N. J. Kettenhofen and M. J. Wood, *Chem. Res. Toxicol.*, 2010, **23**, 1633–1646.
38 D. E. Heppner, Y. M. W. Janssen-Heininger and A. van der Vliet, *Arch. Biochem. Biophys.*, 2017, **616**, 40–46.
39 A. T. Saurin, H. Neubert, J. P. Brennan and P. Eaton, *Proc. Natl. Acad. Sci. U. S. A.*, 2004, **101**, 17982–17987.
40 D. Mansuy and P. M. Dansette, *Arch. Biochem. Biophys.*, 2011, **507**, 174–185.
41 S. Adhikari, R. Crehuet, J. M. Anglada, J. S. Francisco and Y. Xia, *Proc. Natl. Acad. Sci. U. S. A.*, 2020, **117**, 18216–18223.
42 J.-P. R. Chauvin and D. A. Pratt, *Angew. Chem., Int. Ed.*, 2017, **56**, 6255–6259.
43 L. Turell, M. Steglich, M. J. Torres, M. Deambrosi, L. Antmann, C. M. Furdui, F. J. Schopfer and B. Alvarez, *Free Radical Biol. Med.*, 2021, **165**, 254–264.
44 J. T. Petroff, S. M. Omlid, N. Haloi, L. Sith, S. Johnson and R. D. McCulla, *Comput. Theor. Chem.*, 2020, **1189**, 112979.
45 L. A. H. van Bergen, G. Roos and F. De Proft, *J. Phys. Chem. A*, 2014, **118**, 6078–6084.
46 B. Balta, G. Monard, M. F. Ruiz-López, M. Antoine, A. Gand, S. Boschi-Muller and G. Branlant, *J. Phys. Chem. A*, 2006, **110**, 7628–7636.
47 E. Thiriot, G. Monard, S. Boschi-Muller, G. Branlant and M. F. Ruiz-López, *Theor. Chem. Acc.*, 2011, **129**, 93–103.
48 N. W. Pirie, *Biochem. J.*, 1933, **27**, 1181–1188.
49 L. Mao, Z.-S. Liu, C.-H. Huang, T.-S. Tang, H.-Z. Zhang, S.-Y. Chen and B.-Z. Zhu, *Chem. Eng. J.*, 2024, **483**, 148731.
50 Y. Zhao and D. G. Truhlar, *Theor. Chem. Acc.*, 2008, **120**, 215–241.
51 W. J. Hehre, R. Ditchfield and J. A. Pople, *J. Chem. Phys.*, 1972, **56**, 2257–2261.
52 Y. Guo, C. Riplinger, U. Becker, D. G. Liakos, Y. Minenkov, L. Cavallo and F. Neese, *J. Chem. Phys.*, 2018, **148**, 011101.
53 R. A. Kendall, T. H. Dunning and R. J. Harrison, *J. Chem. Phys.*, 1992, **96**, 6796–6806.
54 J. A. Pople, M. Head-Gordon and K. Raghavachari, *J. Chem. Phys.*, 1987, **87**, 5968.
55 M. J. Frisch, J. A. Pople and J. S. Binkley, *J. Chem. Phys.*, 1984, **80**, 3265–3269.
56 T. H. Dunning Jr., *J. Chem. Phys.*, 1989, **90**, 1007.
57 T. Helgaker, W. Klopper, H. Koch and J. Noga, *J. Chem. Phys.*, 1997, **106**, 9639–9646.
58 K. Roos, C. Wu, W. Damm, M. Reboul, J. M. Stevenson, C. Lu, M. K. Dahlgren, S. Mondal, W. Chen, L. Wang, R. Abel, R. A. Friesner and E. D. Harder, *J. Chem. Theory Comput.*, 2019, **15**, 1863–1874.
59 S. Mallick, B. Roy and P. Kumar, *Comput. Theor. Chem.*, 2020, **1187**, 112934.
60 J. Tomasi, B. Mennucci and R. Cammi, *Chem. Rev.*, 2005, **105**, 2999.
61 T. N. Truong and D. G. Truhlar, *J. Chem. Phys.*, 1990, **93**, 1761.
62 Y. Georgievskii and S. J. Klippenstein, *J. Phys. Chem. A*, 2003, **107**, 9776–9781.
63 J. Zheng, S. Zhang and D. G. Truhlar, *J. Phys. Chem. A*, 2008, **112**, 11509–11513.
64 J. M. Anglada, R. Crehuet, S. Adhikari, J. S. Francisco and Y. Xia, *Phys. Chem. Chem. Phys.*, 2018, **20**, 4793–4804.
65 A. J. McGrath, G. E. Garrett, L. Valgimigli and D. A. Pratt, *J. Am. Chem. Soc.*, 2010, **132**, 16759–16761.
66 T. Okuyama, K. Miyake, T. Fueno, T. Yoshimura, S. Soga and E. Tsukurimichi, *Heteroat. Chem.*, 1992, **3**, 577–583.
67 **https://webbook.nist.gov/cgi/cbook.cgi?ID=C62965224&Units=CAL&Mask=8#Thermo-React**.
68 L. Vereecken and J. Peeters, *J. Chem. Phys.*, 2003, **119**, 5159–5170.
69 H. P. Reisenauer, J. Romański, G. Mlostoń and P. R. Schreiner, *Chem. Commun.*, 2013, **49**, 9467–9469.
70 S. Olivella, J. M. Anglada, A. Sole and J. M. Bofill, *Chem. – Eur. J.*, 2004, **10**, 3404–3410.
71 J. M. Anglada, S. Olivella and A. Solé, *J. Am. Chem. Soc.*, 2014, **136**, 6834–6837.
72 J. M. Anglada, M. T. C. Martins-Costa, J. S. Francisco and M. F. Ruiz-López, *J. Am. Chem. Soc.*, 2024, **146**, 14297–14306.
73 J. M. Anglada, *J. Am. Chem. Soc.*, 2004, **126**, 9809–9820.
74 J. M. Anglada, M. T. C. Martins-Costa, J. S. Francisco and M. F. Ruiz-López, *Phys. Chem. Chem. Phys.*, 2019, **21**, 9779–9784.
75 C. H. Switzer and J. M. Fukuto, *Redox Biol.*, 2022, **57**, 102486.
76 U. Barayeu, D. Schilling, M. Eid, T. N. Xavier da Silva, L. Schlicker, N. Mitreska, C. Zapp, F. Gräter, A. K. Miller, R. Kappl, A. Schulze, J. P. Friedmann Angeli and T. P. Dick, *Nat. Chem. Biol.*, 2023, **19**, 28–37.

77 J. M. Mayer, D. A. Hrovat, J. L. Thomas and W. T. Borden, *J. Am. Chem. Soc.*, 2002, **124**, 11142–11147.
78 Q. Zhang, P. Liu, Y. Wang, C. George, T. Chen, S. Ma, Y. Ren, Y. Mu, M. Song, H. Herrmann, A. Mellouki, J. Chen, Y. Yue, X. Zhao, S. Wang and Y. Zeng, *Proc. Natl. Acad. Sci. U. S. A.*, 2023, **120**, e2302048120.
79 L. Tan and Y. Xia, *J. Am. Soc. Mass Spectrom.*, 2013, **24**, 534–542.
80 M. D. Sevilla, D. Becker and M. Yan, *Int. J. Radiat. Biol.*, 1990, **57**, 65–81.
81 Z. Zhang, X. Wang, P. Sivaguru and Z. Wang, *Org. Chem. Front.*, 2022, **9**, 6063–6076.
82 K. L. Durand, X. Ma and Y. Xia, *Analyst*, 2014, **139**, 1327–1330.
83 K. L. Durand, X. Ma and Y. Xia, *Int. J. Mass Spectrom.*, 2015, **378**, 246–254.